Energy Proceedings
Vol 36, 2023
ISSN 2004-2965

Assessing Rooftop Photovoltaic Strategies in Shenzhen's Pingshan District: Cluster-Based Analysis of Energy, Environment, and Economy

Hongjun Li [1], Jing Wang [2], Yingyue Li [1], Yi Zhang [1*]

1 Institute of Future Human Habitats, Tsinghua Shenzhen International Graduate School, Tsinghua University, Shenzhen, 518055, PR China

2 Shenzhen Power Supply Bureau Co., Ltd

(*Corresponding Author: zy1214@sz.tsinghua.edu.cn)

ABSTRACT

Rooftop photovoltaics (RPVs) play a crucial role in reducing urban carbon emissions and aiding the shift toward net-zero energy systems. However, the complexities of urban settings introduce significant variability in RPV costs across different locations and times. This study focuses on the Pingshan District in Shenzhen, a representative example of cities in southern China. The study analyzes geometric characteristics and community types from various urban areas to perform K-means++ clustering. These typical community types are then used to comprehensively assess RPV deployment in terms of energy, environment, and economics. The study provides practical strategies for integrating RPVs, offering insights that contribute to sustainable urban energy transitions.

Keywords: rooftop photovoltaic, K-means++, urban form, cost-benefit analysis, renewable energy strategy

NOMENCLATURE

PV_t	PV generation at time t
E_t	Energy consumption at time t
PV_{s_t}	PV energy consumption at time t
E_{G_t}	Grid energy consumption at time t
$P2G_t$	PV grid feed-in energy at time t
n	The number of samples
X_i, Y_i	The values of corresponding points
$\bar{X}, \bar{Y}$	The sample means
τ_C	The number of concordant pairs
n_d	The number of discordant pairs
$a(i)$	The average dissimilarity (same)
$a(j)$	The average dissimilarity (other)
R_t	RPVs generation revenue
C_t	The cash outflow for t
I_t	The initial investment cost
O_t	The operational costs
M_t	The maintenance expenses
t	Year
$EF_{electricity}$	The carbon emission factor

1. INTRODUCTION

In the context of addressing the global climate crisis, the adoption of carbon neutrality policies has emerged as an urgent measure to control carbon dioxide emissions [1]. Against this backdrop, photovoltaic (PV) technology has emerged as a pivotal means for China to rapidly reduce its reliance on fossil fuels [2]. Urban areas, characterized by their dense architectural layout, have been identified as a prime domain for the large-scale implementation of additional PV power generation. In comparison to traditional centralized PV systems, this approach effectively mitigates issues of significant solar energy wastage. Distributed Photovoltaic (DPV) systems, due to their widespread applicability, lower peak energy demands, and reduced transmission issues, have garnered significant favor [3].

Nevertheless, despite the manifold advantages of DPV systems, the heterogeneity of urban spaces presents certain challenges [4]. Disparate urban morphologies across different regions result in divergent shading patterns and energy consumption profiles, consequently influencing the efficacy of PV deployment. Non-strategic PV installations may potentially impede the national carbon neutrality agenda. Therefore, the formulation of PV deployment strategies necessitates a comprehensive consideration of regional disparities and characteristics.

This is a paper for the 9th Applied Energy Symposium: Low Carbon Cities and Urban Energy Systems (CUE2023), Sep. 2-7, 2023, Matsue & Tokyo, Japan.

The expansion of distributed photovoltaics requires targeted strategic guidance to fully unleash its potential. Consequently, numerous researchers have conducted in-depth studies on photovoltaic deployment strategies from various perspectives, including environmental, technological, economic, and social dimensions. Some have examined the trade-off between cost-effectiveness and equitable regional distribution inherent in the deployment of distributed photovoltaics [5]. Others have pursued distinct approaches to attain national photovoltaic objectives, namely, minimizing the number of rooftops required to meet national targets while concurrently maximizing regional self-sufficiency, all in alignment with the broader national photovoltaic agenda [6]. Certain studies have focused on economic strategies, employing fundamental economic theories such as net present value (NPV), payback period, and internal rate of return (IRR), to conduct an economic comparative analysis of residential solar photovoltaic systems across various provinces [7,8]. There have also been studies exploring the potential benefits of deploying solar photovoltaic systems on urban rooftops, with a strategic emphasis on maximizing the reduction of the urban heat island effect [9].

To adeptly formulate and evaluate urban energy strategies, given the escalating volume of urban big data, the utilization of machine learning algorithms for data simplification has emerged as a discernible trend in research. Research endeavors have employed multiple linear regression (MLR) and Akaike Information Criterion (AIC) to simulate annual heat demand or peak heat demand, accomplished through clustering of building attributes [10]. Another study leveraged random forest regression in conjunction with heterogeneous geospatial data sources to identify rooftop areas. Subsequently, K-means++ clustering analysis was conducted using rooftop area, solar radiation, and grid emissions as features to unveil the heterogeneity in carbon emission reduction potential across distinct cities [11]. Furthermore, a study initially utilized Multi-Layer Perceptron (MLP) to ascertain annual electricity generation and peak power of photovoltaic panels on residential rooftops. Subsequently, Support Vector Regression (SVP) was employed for data classification, facilitating finer-grained energy planning [12]. Additionally, the utilization of the DBSCAN clustering algorithm, in combination with infrastructure data from OpenStreetMap, led to the construction of a global solar photovoltaic installation dataset [13].

Following the utilization of machine learning algorithms to analyze simplified urban datasets, more rapid assessments can be conducted regarding photovoltaic deployment in aspects encompassing energy, environment, and economics. Previous research has approached the analysis and evaluation of urban photovoltaics from various angles, thereby shaping photovoltaic deployment strategies. Several studies have undertaken comprehensive evaluations of the economic benefits of distributed photovoltaics by considering factors such as total project investment, electricity generation, and transaction prices across 344 prefecture-level cities in China [14]. Leveraging key metrics such as Levelized Cost of Energy (LCOE) and Internal Rate of Return (IRR) based on the technological and cost foundations of photovoltaic deployment, another study conducted an in-depth economic analysis of China's distributed photovoltaic industry [15]. Additionally, through estimations of technological potential and financial feasibility analysis, a study examined and assessed the economic benefits, environmental impact, and health effects associated with the promotion of household solar photovoltaics at the urban level [16].

The current study has made significant strides in comprehensively formulating photovoltaic deployment strategies at a macroscopic level. However, there has been limited research focusing on the simplification of urban big data through machine learning techniques to address urban morphological characteristics, followed by the integration of indicators such as IRR and LCOE to determine the sequence of photovoltaic deployment at the urban community scale.

In this paper, we initially obtained road network and building data through OpenStreetMap (OSM). Subsequently, we subdivided the city into communities of approximate sizes, extracting community types and morphological parameters. Photovoltaic and energy consumption simulations were conducted for each community. Employing the k-means++ clustering technique, six representative community types were identified. Building upon this framework, an analysis encompassing energy, environment, and economics was conducted. Ultimately, the photovoltaic deployment strategy for the Pingshan District was derived.

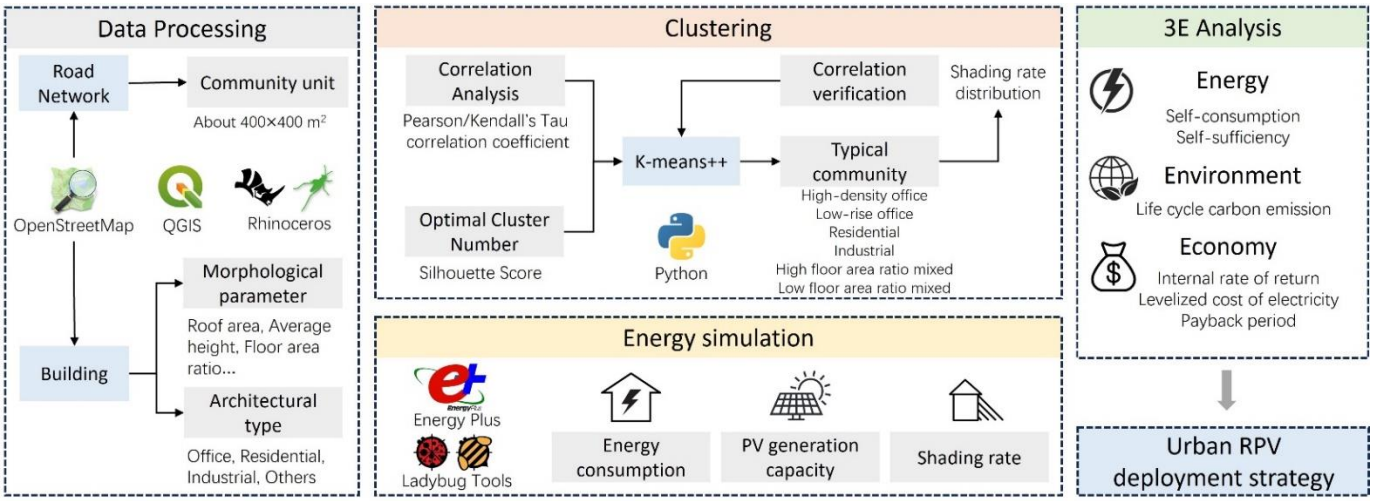

Fig. 1 Framework for urban RPV deployment strategy

2. METHODOLOGY

2.1 *Overview of the framework for urban RPVs deployment strategy*

The overarching research framework is depicted in Fig. 1. Initially, utilizing OpenStreetMap (OSM) data for road networks and building information, the district is segmented into 317 communities.

Morphological parameters are then extracted from these locales, enabling the simulation of RPVs capacity and energy consumption through Energy Plus. Employing the K-means++ algorithm based on these morphological attributes, six prototypical communities are delineated.

Ultimately, employing indicators encompassing self-sufficiency rates, carbon emissions, and internal rate of return, a comprehensive trilateral analysis is undertaken, evaluating urban RPVs deployment strategies across energy, environmental, and economic domains.

2.2 Data Processing

The data processing procedure commenced by extracting road network and building information for the Pingshan District of Shenzhen using OpenStreetMap. Subsequently, leveraging the Grasshopper plugin within Rhinoceros, the district was partitioned into community units of approximately 400 by 400 square meters each, based on the road network. Morphological characteristics for each community unit were then computed and exported.

These characteristics encompassed parameters such as average building height, building footprint, roof area, building area, and building count. Additionally, the community units were categorized into various types, including office, residential, industrial, and other. These processed data were organized into a comprehensive data matrix for further analysis.

In addition, to conduct a targeted investigation into photovoltaic deployment strategies within Shenzhen, we conducted a market survey for the initial investment in a 10 kW photovoltaic system, as presented in Table 1.

Furthermore, we obtained the desulfurized coal electricity price and government subsidy price for the PV grid connection in Shenzhen, which is 0.453 CNY/kWh and 0.3 CNY/kWh, respectively.

The carbon emission factor was determined as 0.3748 kgCO2/kWh. These data, along with the tiered electricity pricing structure in Shenzhen, will underpin the environmental and economic indicator calculations for photovoltaic deployment in this study.

Table 1
Investigation of rooftop photovoltaic (10 kW) prices.

Content	Price
Grid-Connected Inverter	6,300 CNY
36V Monocrystalline Silicon Panel	32,000 CNY
AC Distribution Box	1,500 CNY
Photovoltaic Cabling	1,500 CNY
RPVs Mounting Structure	8,250 CNY
Construction Costs	5,000 CNY
O&M Costs	500 CNY/year

2.3 Energy simulation

Following the acquisition of geometric parameters and building types, we proceeded to conduct comprehensive photovoltaic energy yield simulations and building energy consumption simulations for all structures within each community unit. This was achieved using the Ladybug Tools plugin, which is based on Energy Plus. Subsequently, through meticulous data processing, we obtained

photovoltaic generation, overall energy consumption, and shading rates for a total of 317 community units.

2.4 K-means++ clustering

To streamline the extensive workload introduced by the vast building dataset during urban energy simulation, this study opted to directly extract geometric parameters and types for each community. Subsequently, clustering was employed to group these community units, whereby a small number of representative community types were chosen to stand for similar-natured counterparts. This approach facilitated a comprehensive assessment of photovoltaic deployment.

Upon obtaining the generated data for photovoltaics, energy consumption, and shading rates for each community, along with the statistically derived community types and geometric parameters, an initial correlation analysis was performed on all data using the Pearson and Kendall's Tau correlation coefficients [17,18], as depicted in Equation (1, 2).

$$r = \frac{\sum_{i=1}^{n}(X_i - \bar{X})(Y_i - \bar{Y})}{\sqrt{\sum_{i=1}^{n}(X_i - \bar{X})^2}\sqrt{\sum_{i=1}^{n}(Y_i - \bar{Y})^2}} \quad (1)$$

where n represents the number of samples, X_i and Y_i denote the values of corresponding points, while $\bar{X}$ and $\bar{Y}$ stand for the sample means.

$$\tau_C = \frac{2(n_c - n_d)}{n^2 \frac{(m-1)}{m}} \quad (2)$$

where, n_c represents the number of concordant pairs, n_d represents the number of discordant pairs, r and c denote the number of rows and columns, while m represents the minimum value between r and c.

Before employing k-means++ clustering [19], the optimal number of clusters based on the geometric parameters of the 317 communities was determined using the silhouette coefficient method [20], as depicted in Equation (3) This step was taken to achieve improved clustering performance.

$$S(i) = \frac{b(i) - a(i)}{\max\{a(i), b(i)\}} \quad (3)$$

where, $b(i)$ represents the average dissimilarity of vector i to the other points within the same cluster, $a(i)$ represents the minimum average dissimilarity of vector i to the points in other clusters.

Following the clustering of six representative community types, this study conducted a comparative analysis of the photovoltaic shading distribution across the buildings within each of the six typical communities. This analysis served as a supplementary validation of the clustering correlations.

2.5 Energy–Environment–Economy (3E) Analysis

This study comprehensively evaluates urban rooftop photovoltaic deployment from three perspectives: energy, environment, and economics, for the six representative community types extracted through clustering, by integrating photovoltaic generation and building energy consumption data.

2.5.1 Energy Performance

In this study, the Ladybug Tools framework was employed to simulate the hourly shading-dependent photovoltaic energy yield and hourly energy consumption for all buildings in the Pingshan District. The simulation process involved defining building types and geometric parameters. It was assumed that all buildings engaged in a self-consumption behavior, utilizing surplus electricity for grid feed-in. Consequently, building energy usage was categorized into three distinct classes: photovoltaic self-consumption, grid electricity supply, and photovoltaic grid feed-in.

$$PV_{s_t} = min(E_t, PV_t) \quad (4)$$

$$E_{G_t} = E_t - PV_{s_t} \quad (5)$$

$$P2G_t = PV_t - PV_{s_t} \quad (6)$$

where, PV_t, E_t, PV_{s_t}, E_{G_t}, and $P2G_t$ respectively denote the PV generation, energy consumption, PV energy consumption, grid energy consumption, and PV grid feed-in energy for the community at time t.

$$\text{Self consumption } (\%) = \frac{\sum_{t=1}^{T} PV_{s_t}}{\sum_{t=1}^{T} PV_t} \times 100(\%) \quad (7)$$

$$\text{Self sufficiency } (\%) = \frac{\sum_{t=1}^{T} PV_{s_t}}{\sum_{t=1}^{T} E_t} \times 100(\%) \quad (8)$$

where, T represents the total number of hours in a year, which is 8760.

2.5.2 Environmental Performance

Although rooftop photovoltaics can reduce reliance on fossil-fuel-based electricity generation and subsequently mitigate carbon emissions, a comprehensive life-cycle perspective reveals that carbon dioxide emissions are generated during the production, transportation, and maintenance of photovoltaic components and rooftop installations. While the carbon emissions reduction focus of photovoltaics predominantly pertains to the electricity generation phase within the power system, neglecting

other life-cycle stages[21], this study primarily calculates carbon emissions during the operational phase.

$$EM = E_t \times EF_{electricity} \times \mathrm{y} \quad (9)$$

where EM represents the life-cycle carbon emissions of RPVs, EF signifies the carbon emission factor, and y denotes the operational lifespan.

2.5.3 Economic Performance

Urban photovoltaic deployment requires significant economic support. In this study, rooftop photovoltaics are assumed to account for 100% of the capital investment. From an investment perspective, three economic indicators, namely IRR [22], LCOE [14], and Payback Period were chosen to assess the benefits of photovoltaic deployment. The tiered electricity pricing structure is based on the electricity price table of Shenzhen. The initial photovoltaic investment is referenced from market prices, and a discount rate of 6.5% is employed for present value calculations.

$$R_t = PV_{s_t} P_1 + P2G_t(P_2 + P_3) \quad (10)$$

where, R_t represents RPVs generation revenue, P_1, P_2 and P_3 respectively denote the converted tiered electricity price, grid electricity price, and government subsidy.

$$LCOE = \frac{\sum_{t=o}^{T}(I_t + O_t + M_t + F_t)/(1+r)^t}{\sum_{t=0}^{T} Q_t/(1+r)^t} \quad (11)$$

where, I_t represents the initial investment cost, O_t, M_t and F_t correspondingly stand for operational costs, maintenance expenses, and interest outlays. r represents the discount rate.

$$NPV(r) = \sum_{t=0}^{T}(R_t - C_t)(1+r)^{-t} = 0 \quad (12)$$

where, C_t represents the cash outflow for t, when the $NPV(r)$ reaches zero, the calculated value of r represents the IRR.

3. RESULTS

3.1 Clustering of Typical Communities

3.1.1 Correlation Analysis

In this study, a comprehensive correlation analysis was conducted on thirteen distinct feature parameters, including PV generation, community energy consumption, PV shading rate, average building height, building footprint, roof area, floor area ratio, building area, building count, and building types (office, residential, industrial, others). Both Pearson and Kendall's Tau correlation coefficient tests were employed for this purpose.

The findings revealed significant correlations among certain parameters. PV generation exhibited a strong positive correlation with roof area (0.98) and a relatively strong correlation with building area (0.89) and building number (0.77). It should be noted that the non-equal correlation value between PV generation and roof area (less than 1) is attributed to varying shading conditions caused by different buildings within urban units. The PV shading rate displayed moderate correlations with floor area ratio (0.26) and average building height (0.22), indicating their notable influence. Notably, the building area demonstrated a substantial correlation with PV generation (0.68), yet an even stronger correlation with community energy consumption (0.71), suggesting the impact of shading rate on PV generation. Additionally, building count exhibited a moderate correlation with PV generation (0.54) and a significant correlation with community energy consumption (0.71), attributed to the increase in energy consumption associated with greater building quantities.

Furthermore, the analysis highlighted the variability in the degree of association between different building types and both PV generation and community energy consumption. These research outcomes underscore the intricate interplay between various parameters and support the use of clustering based on geometric parameters and types to simplify complex urban datasets.

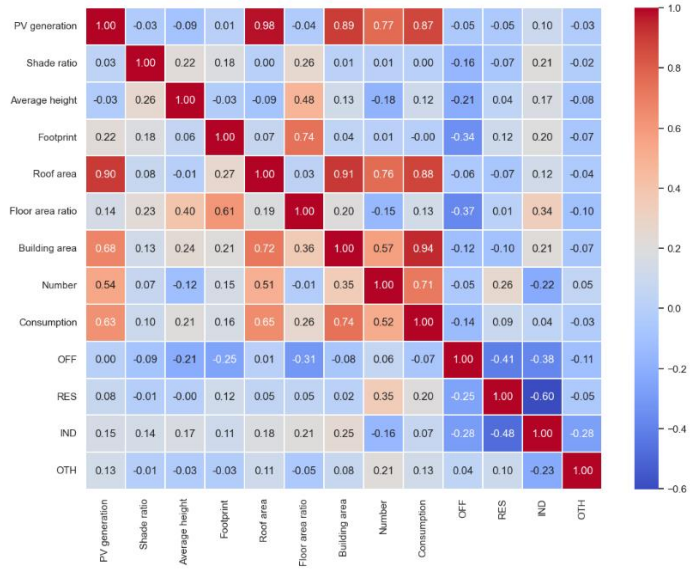

Fig. 2 The Combined Pearson and Kendall's Tau Correlation between energy consumption, PV generation, shading rates, and morphological parameters.

3.1.2 Optimal Number of Clusters

In this study, a rigorous validation process was employed utilizing the elbow method, Calinski-Harabasz score, and silhouette coefficient method to mutually

corroborate the optimal number of clusters for the given dataset under the k-means++ algorithm. The analysis converged to a consensus, indicating that the most suitable clustering configuration for the data was determined to be six, as depicted in Fig 3.

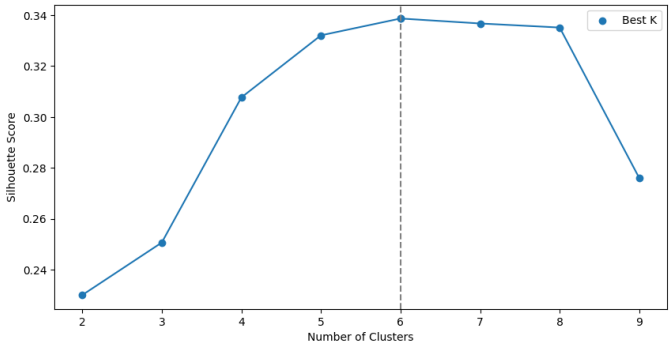

Fig. 3 The calculation of the silhouette coefficient to determine the optimal number of clusters.

3.1.3 Six Representative Community Types

Post-clustering analysis revealed the emergence of six distinct typologies within the community dataset. Observing Fig 4, it is evident that disparate distribution patterns exist among these categories, thereby attesting to the efficacy of the clustering outcomes. Notably, Fig 5 illustrates the representative nature of the typical communities in each category and their alignment with other communities within the six identified clusters. This alignment underscores the ability of the prototypical communities to effectively characterize others based on geometric parameters and types. Furthermore, Table 2 provides a comprehensive summary of the various feature indicators characterizing the six identified typologies.

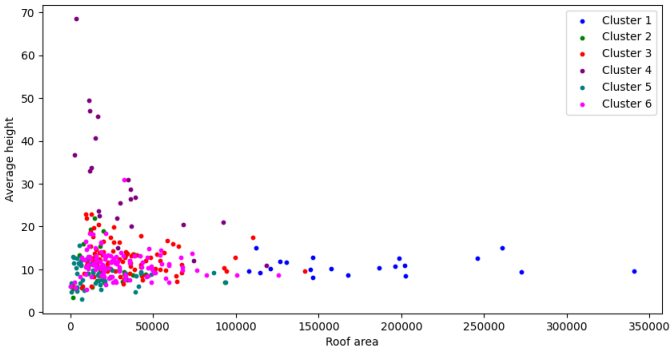

Fig. 4 The outcomes of K-means++ clustering.

From the insights drawn from Fig 5, it becomes apparent that the first and second categories are dominated by mixed-use buildings, the third category is predominantly industrial, and the fourth and fifth categories are predominantly office-oriented, with the sixth category being residential. An examination of Table 2 in conjunction with these findings reveals notable distinctions. Despite both the first and second categories being characterized by mixed-use buildings, the former exhibits greater average building height, significantly larger roof area, and floor area ratio compared to the latter. This implies the potential subdivision of these categories into high-density and low-density mixed-use communities. Similarly, the fourth and fifth categories, both centered around office usage, reveal a substantial contrast in terms of average building height and floor area ratio, with the former approximately six times that of the latter. This discrepancy suggests that the fourth category represents high-rise office communities.

The alignment between clustering outcomes and real-world observations serves to reaffirm the validity of employing geometric parameters and building types for the simplification of urban datasets, thus further validating the rationale of the clustering methodology.

3.1.4 Correlation Validation

Following the clustering analysis, we opted to employ photovoltaic degradation rate as an assessment metric to explore the distribution of photovoltaic degradation rates across the six identified community types. Observations of the outcomes reveal discernible distinctions in photovoltaic degradation rates among different community types. Notably, the interquartile range (IQR) values for each community type exhibit relatively small differences, with the IQRs of five categories all being less than 7%. This phenomenon indicates that within each community type, the dispersion of photovoltaic degradation rates is minimal, thereby highlighting distinct clustering characteristics. Additionally, significant differences are observed in the median photovoltaic degradation rates across the various community types, further corroborating the distinctiveness between different category communities.

These findings further corroborate the effectiveness of utilizing geometric parameters and building types for clustering in capturing community attributes.

3.2 Energy Simulation of Typical Communities

Upon acquiring hourly simulated photovoltaic and energy data, this study proceeded to extract weekly time windows for each of the six typical community types across different seasons of the year. This observation sought to discern the behaviors of diverse community categories concerning PV generation and energy consumption.

As depicted in Fig 7, it is evident that the photovoltaic curve trends for the six community types exhibit approximate similarity, with distinctions primarily manifesting in terms of generation capacity. This

Table 2
Distinct characteristics of the six typical communities.

Cluster	Average height	Footprint	Roof area	Floor area ratio	Building area	Number	OFF	RES	IND	OTH
1	9.625	0.1341	202239.2	1.9987	2050100	1177	23.29	39.91	5.76	31.04
2	3.375	0.0215	93180.15	0.1179	659813.4	502	30.17	23.40	0.45	45.98
3	6.000	0.0177	19477.53	5.0722	268887	67	9.44	0.00	90.56	0.00
4	36.750	0.0402	36428.16	9.0768	992907.5	36	88.13	0.00	11.87	0.00
5	6.000	0.0011	19056.19	1.5813	140993	77	82.76	0.24	0.00	17.00
6	6.000	0.0289	46395.29	3.7268	588217.1	432	3.64	91.71	3.98	0.66

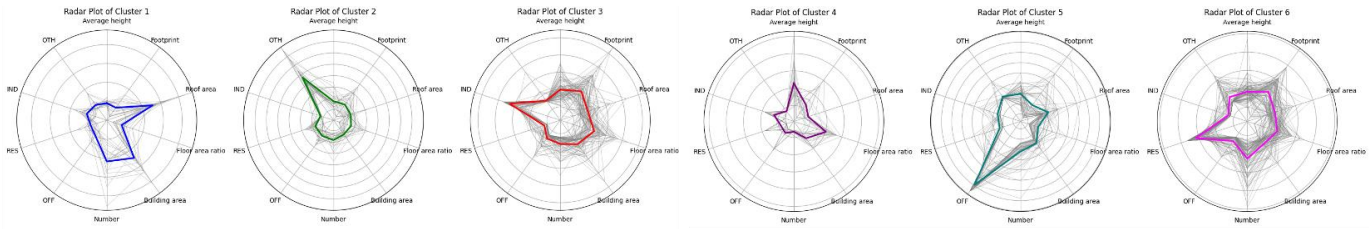

Fig. 5 The clustering results reveal distinctive feature distributions among the six typical communities.

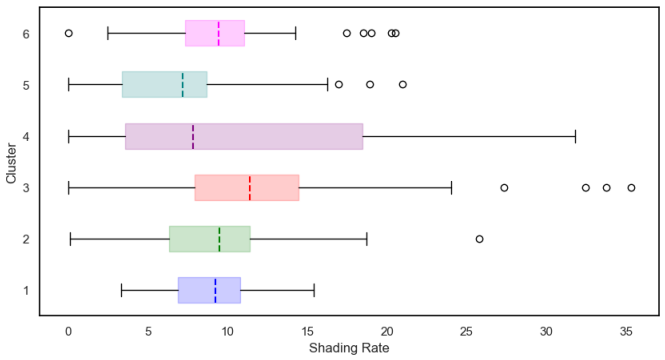

Fig. 6 PV shading distribution across buildings in the six community types.

phenomenon is attributed to the fact that, within the same climatic context, photovoltaic conditions across various community types are primarily influenced by minimal variations in shading coefficients. The variability in generation capacity arises from the distinct characteristics of building quantities and roof areas among different community types. In contrast, the energy consumption curves for different community types consistently exhibit a trend where energy consumption during the summer surpasses that during the winter. This trend is reflective of Shenzhen's geographical location in a subtropical region of China, where the summer season necessitates heightened air conditioning demand and consequently increased energy consumption.

Moreover, notable variations exist in the structural form of energy consumption curves among different community types. As previously analyzed, the first and second community types, characterized by mixed building compositions, exhibit less distinct features in their energy consumption curves due to their diverse building typologies. However, both types tend to have higher energy consumption on weekdays compared to weekends. The lower density of the second type contributes to a relatively smaller magnitude of energy consumption peaks within its curve.

Additionally, the photovoltaic curve of this type overlaps with the energy consumption curve during certain time intervals, signifying the self-consumption of photovoltaic energy. The third community type, predominantly comprising industrial structures, displays discernible disparities between energy consumption on weekdays and weekends, and exhibits a bimodal daily consumption curve, reflective of machinery operation and associated energy consumption during morning and afternoon production hours.

The fourth and fifth community types, dominated by office buildings, similarly exhibit lower energy consumption on weekdays. The primary differentiation between these two types lies in their structural heights, with the fourth type comprising high-rise office structures, resulting in considerably lower photovoltaic generation capacity relative to building consumption. In contrast, the fifth type's lower average building height enables photovoltaic generation to partially cover building energy demand under favorable sunlight conditions. Moreover, due to the coexistence of residential structures within the fifth type, the bimodal energy consumption pattern daily is less pronounced compared to the fourth type. Finally, the sixth community type, characterized by residential

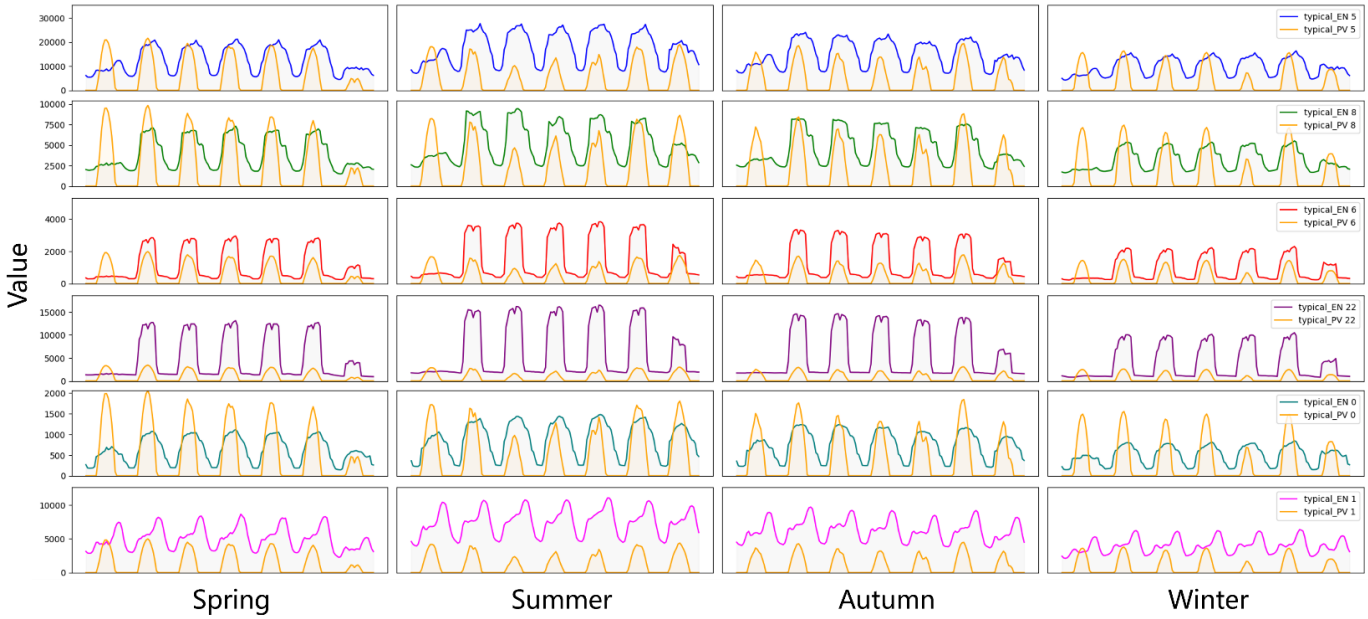

Fig. 7 The photovoltaic and energy consumption curves of six typical communities during different seasons throughout the year.

buildings, attains its peak energy consumption during evening hours, with a minor peak observed in the early morning. This pattern is attributed to residential occupants returning home and initiating appliance usage in the evenings, with a subsequent modest increase in energy consumption following morning activities.

The qualitative assessment of hourly energy consumption diagrams serves to characterize the interplay between photovoltaic generation and energy consumption across the six typical community types. Furthermore, this exercise enhances our understanding of the distinctive variations existing among different community categories. Consequently, the feasibility of the undertaken clustering analysis is reaffirmed.

3.3 Energy–Environment–Economy (3E) Analysis

3.3.1 Energy Performance

Following the simulation of hourly photovoltaic generation and energy consumption for the typical community clusters, under the assumption of a self-consumption and surplus electricity grid-feeding strategy, this study classifies energy into three categories: photovoltaic self-consumption, grid electricity supply, and photovoltaic grid-feeding. Subsequently, the self-consumption rate and self-sufficiency rate for each community category are computed.

The self-consumption rate, defined in this study as the proportion of photovoltaic self-consumed energy to total photovoltaic generation, serves as an indicator of system efficiency. A higher self-consumption rate signifies greater energy self-sufficiency and reduced reliance on the external electricity supply. By comparing self-consumption rates, it is evident that the sixth community type, dominated by residential buildings, achieves a self-consumption rate of 100%. This indicates that residential communities can effectively utilize photovoltaic-generated electricity, thereby minimizing surplus grid-feeding and showcasing promising economic potential in terms of energy performance. High-rise office-dominated communities attain a self-consumption rate of 98.6%, primarily due to the relatively small energy demand of high-rise buildings concerning their photovoltaic generation capacity.

The self-sufficiency rate, defined as the proportion of photovoltaic self-consumed energy to total building electricity consumption, is another key metric analyzed in this study. It is noteworthy that the self-sufficiency rates across various community types are relatively low. Specifically, the self-sufficiency rate for high-rise office-dominated communities is 10.1%, indicating significant room for improvement in flexible energy utilization within this community. Comparatively higher self-sufficiency is observed in the fifth community type, predominantly due to the overlapping nature of its photovoltaic and energy consumption curves.

3.3.2 Environmental Performance

In this study, the environmental performance of photovoltaic deployment was assessed using a life cycle

Table 3
Energy, Environmental, and Economic Evaluation Indicators for the Six Representative Community Types.

Cluster	PV/kWh	EN/kWh	SC	SS	CO2/kg	R_t	IRR	Payback Period	LCOE	Shading rate
1	26996320	116663900	0.981	0.227	43725624	2047.57	0.0893	11	0.6891	9.3
2	12323554	357303330	0.932	0.321	13391728	935.04	0.0882	11	0.6955	10.1
3	2482435	9911961	0.943	0.236	3715003	188.09	0.0836	12	0.7217	13.4
4	4304789	41664294	0.986	0.101	15615777	326.42	0.0749	13	0.7784	19.7
5	2576520	5789079	0.898	0.400	2169747	195.71	0.0911	11	0.6803	8.1
6	6244251	48755676	1	0.128	18273627	473.35	0.0903	11	0.6834	8.5

carbon emissions approach. The carbon emissions of different community types exhibit a proportional relationship with their energy consumption. Notably, the highest carbon emissions are observed in the first community type, characterized by high-density mixed-use buildings, which annually generate 43,725,623.98 kg of carbon dioxide. Conversely, the lowest carbon emissions are found in the low-rise office-dominated community, with an annual carbon emission of 2,169,746.962 kg, representing approximately one-twentieth of the emissions from the first community type.

3.3.3 Economic Performance

In this study, it is assumed that the investment in RPVs deployment constitutes 100% of the capital, thus not considering bank loans or financing. The evaluation of the economic viability of PV deployment in different types of communities is conducted through three key indicators: IRR, LCOE, and Payback Period. Specific numerical values are provided in Table 3, the main conclusions drawn from the analysis are as follows: The IRR for the community dominated by high-rise office buildings is calculated at 7.4%, which is below the standard benchmark of 8% often used in rooftop PV investment assessment. This suggests a relatively lower return on investment for the PV project in this context. The LCOE values for all typical community types are below 0.9504 CNY/kWh, which is the average weighted electricity price for Shenzhen during 2022-2023, implying that distributed PV electricity costs are lower than the electricity prices paid by local industrial and commercial users. However, these values are still higher than the price of desulfurized coal (0.453 CNY/kWh).

This indicates that, from the perspective of power generation, distributed PV electricity costs remain higher than the local desulfurized coal price under the current PV cost and technological conditions, posing certain challenges to achieving grid parity on the generation side.

The payback periods for all community types exceed 10 years, indicating that the investment cost of PV deployment in Shenzhen remains relatively high. Notably, the community dominated by high-rise office buildings exhibits the longest payback period of 13 years.

Given similar climate conditions, local electricity prices, and subsidies, the economic performance of PV deployment in the same region is greatly influenced by the geometric parameters of the community. Average building height and plot ratio result in varying levels of shading, leading to reductions in PV output and consequently affecting the economic feasibility of PV deployment.

3.3.4 RPVs Deployment Strategy

The 3E analysis encompasses a range of evaluation metrics for RPVs deployment, among which self-consumption rate, carbon emissions, and IRR hold significance. In this study, these indicators serve as references for the proposed PV deployment strategy in the Pingshan district. Given the substantial reliance on economic investment for PV implementation, IRR stands as the foremost consideration.

The 3E performance distribution across six typical communities is depicted in Fig 8. It is evident that the fourth category, characterized by high-rise office-dominated communities, exhibits the lowest IRR and comparatively higher carbon emissions. Thus, it is deemed suitable for subsequent deployment phases. Conversely, the fifth category, comprising low-rise office-dominated communities, showcases the highest IRR at 9.1% and the lowest carbon emissions, underscoring its priority for initial deployment. Furthermore, residential-dominated communities present a relatively substantial IRR and attain a self-consumption rate of 100%, warranting a preferential deployment approach.

The first and second categories exhibit closely proximate IRR values. However, the former exhibits significantly higher carbon emissions compared to the latter. Consequently, the deployment sequence for low-density mixed-use communities takes precedence over high-density counterparts.

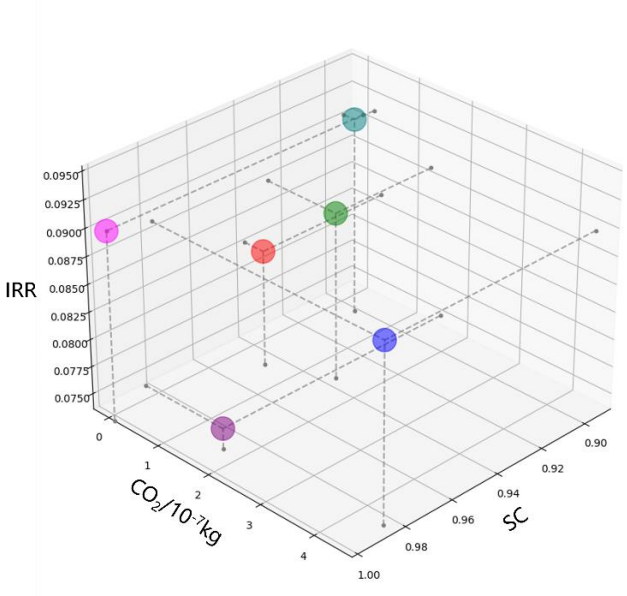

Fig. 8 Self-Consumption Rate, Carbon Emissions, and IRR for the Six Representative Community Types.

4. DISCUSSION AND LIMITATION

The present study has yet to incorporate alternative investment modalities for RPVs installations, such as operational leasing models, zero-down payment PV loan models, and rooftop rental schemes. Future investigations may delve into delineating the optimal investment approach corresponding to various urban units.

The current scope of urban inquiry encompasses the Ping Shan district of Shenzhen. Subsequent endeavors could extend the methodological framework delineated herein to encompass the entirety of Shenzhen. This expansion could leverage machine learning algorithms to streamline data processing and employ the 3E analysis for formulating RPVs deployment strategies. Moreover, a comparative analysis could be pursued, involving Beijing, a city characterized by distinct climatic conditions, local electricity tariffs, and urban morphologies, to enrich the investigation by contrasting North and South China urban contexts.

The existing evaluative model confines itself to the realms of energy, environment, and economics. Future research avenues may encompass a broader spectrum, introducing social dimensions. This incorporation could encompass gauging the residents' inclinations toward PV adoption across disparate communities, augmenting the analysis with a 3ES model, thus fostering a more comprehensive and unbiased conclusion.

5. CONCLUSION

This study extracted geometric parameters and typologies of various communities to perform clustering, subsequently utilizing representative typologies to conduct comprehensive evaluations of RPVs deployment. The main conclusions derived from this analysis are as follows:

1. Through correlation analysis, validation, and clustering results, it was demonstrated that urban units can be clustered based on their geometric parameters and typologies. This enables the representation of vast urban data through typical units, simplifying the study of urban energy.

2. Notable discrepancies exist in PV and energy consumption curves among the six typical community categories, thereby corroborating actual energy consumption patterns.

3. Regarding energy aspects, residential communities exhibit a 100% self-consumption rate, indicating intrinsic energy usage and economic potential. However, all building types have a self-sufficiency rate of less than 50%, indicating considerable flexibility in energy consumption.

4. Environmental implications reveal that carbon emissions are primarily linked to building energy consumption, with high-density mixed-use communities registering the highest emissions at 43,725,623.98 kg per year.

5. From an economic perspective, the IRR for high-rise office-dominated communities is 7.4%, implying a relatively lower investment return. Conversely, other community types exceed an 8% IRR, aligning with standard metrics in rooftop PV investment. The LCOE ranges between 0.453 CNY/kWh and 0.9504 CNY/kWh, suggesting end-users can access cost-parity given current technology and cost levels. However, achieving grid parity on the generation side remains challenging.

6. Utilizing representative typologies, the study determined a sequence for RPVs deployment in 317 community units within Shenzhen's Ping Shan district. The recommended order is to commence with low-rise office-dominated communities, followed by residential-dominated communities, low-density mixed-use communities, high-density mixed-use communities, industrial-dominated communities, and ultimately high-rise office-dominated communities.

This study elucidates efficacious approaches for the integration of RPVs, imparting valuable insights conducive to the pursuit of sustainable urban energy transitions.

ACKNOWLEDGEMENT

Key Research Program of China Southern Power Grid (090000KK52210134); Scientific Research Start-up Funds of Tsinghua Shenzhen International Graduate School (QD2021007N).

DECLARATION-OFINTERESTSTATEMENT

The authors declare that they have no known competing financial interests or personal relationships that could have appeared to influence the work reported in this paper. All authors read and approved the final manuscript.

REFERENCE

[1] Mallapaty S. How China could be carbon neutral by mid-century. Nature 2020;586:482–3. https://doi.org/10.1038/d41586-020-02927-9.

[2] Accelerating the energy transition towards photovoltaic and wind in China | Nature n.d. https://www.nature.com/articles/s41586-023-06180-8 (accessed August 14, 2023).

[3] Manfren M, Caputo P, Costa G. Paradigm shift in urban energy systems through distributed generation: Methods and models. Applied Energy 2011;88:1032–48. https://doi.org/10.1016/j.apenergy.2010.10.018.

[4] Spatial heterogeneity of urban–rural integration and its influencing factors in Shandong province of China | Scientific Reports n.d. https://www.nature.com/articles/s41598-022-18424-0 (accessed August 14, 2023).

[5] Distributional trade-offs between regionally equitable and cost-efficient allocation of renewable electricity generation - ScienceDirect n.d. https://www.sciencedirect.com/science/article/pii/S0306261919314114?via%3Dihub (accessed August 14, 2023).

[6] Walch A, Rüdisüli M. Strategic PV expansion and its impact on regional electricity self-sufficiency: Case study of Switzerland. Applied Energy 2023;346:121262. https://doi.org/10.1016/j.apenergy.2023.121262.

[7] Sow A, Mehrtash M, Rousse DR, Haillot D. Economic analysis of residential solar photovoltaic electricity production in Canada. Sustain Energy Technol Assess 2019;33:83–94. https://doi.org/10.1016/j.seta.2019.03.003.

[8] Economic analysis of residential solar photovoltaic systems in China - ScienceDirect n.d. https://www.sciencedirect.com/science/article/pii/S0959652620353427?via%3Dihub (accessed August 14, 2023).

[9] Pricing the urban cooling benefits of solar panel deployment in Sydney, Australia | Scientific Reports n.d. https://www.nature.com/articles/srep43938 (accessed August 14, 2023).

[10] A building clustering approach for urban energy simulations - ScienceDirect n.d. https://www.sciencedirect.com/science/article/pii/S0378778819313271 (accessed August 14, 2023).

[11] Carbon mitigation potential afforded by rooftop photovoltaic in China | Nature Communications n.d. https://www.nature.com/articles/s41467-023-38079-3 (accessed August 14, 2023).

[12] Rooftop Detection for Planning of Solar PV Deployment: A Case Study in Abu Dhabi | SpringerLink n.d. https://link.springer.com/chapter/10.1007/978-3-319-13290-7_11 (accessed August 14, 2023).

[13] Harmonised global datasets of wind and solar farm locations and power | Scientific Data n.d. https://www.nature.com/articles/s41597-020-0469-8 (accessed August 14, 2023).

[14] City-level analysis of subsidy-free solar photovoltaic electricity price, profits and grid parity in China | Nature Energy n.d. https://www.nature.com/articles/s41560-019-0441-z (accessed August 14, 2023).

[15] Technology, cost, economic performance of distributed photovoltaic industry in China - ScienceDirect n.d. https://www.sciencedirect.com/science/article/pii/S1364032119302825 (accessed August 14, 2023).

[16] Chen H, Chen W. Status, trend, economic and environmental impacts of household solar photovoltaic development in China: Modelling from subnational perspective. Applied Energy 2021;303:117616. https://doi.org/10.1016/j.apenergy.2021.117616.

[17] Jebli I, Belouadha F-Z, Kabbaj MI, Tilioua A. Prediction of solar energy guided by pearson correlation using machine learning. Energy 2021;224:120109. https://doi.org/10.1016/j.energy.2021.120109.

[18] Muñoz-Pichardo JM, Lozano-Aguilera ED, Pascual-Acosta A, Muñoz-Reyes AM. Multiple Ordinal Correlation Based on Kendall's Tau Measure: A Proposal. Mathematics 2021;9:1616. https://doi.org/10.3390/math9141616.

[19] Bahmani B, Moseley B, Vattani A, Kumar R, Vassilvitskii S. Scalable K-Means++ 2012. https://doi.org/10.48550/arXiv.1203.6402.

[20] Bagirov AM, Aliguliyev RM, Sultanova N. Finding compact and well-separated clusters: Clustering using silhouette coefficients. Pattern Recognit 2023;135:109144. https://doi.org/10.1016/j.patcog.2022.109144.

[21] Wang M, Mao X, Gao Y, He F. Potential of carbon emission reduction and financial feasibility of urban rooftop photovoltaic power generation in Beijing. J Clean Prod 2018;203:1119–31. https://doi.org/10.1016/j.jclepro.2018.08.350.

[22] Wolske KS, Todd-Blick A, Tome E. Increasing the reach of low-income energy programmes through behaviourally informed peer referral. Nat Energy 2023:1–9. https://doi.org/10.1038/s41560-023-01298-5.